Research Square

Preprints are preliminary reports that have not undergone peer review.
They should not be considered conclusive, used to inform clinical practice,
or referenced by the media as validated information.

Model-based estimation of microbial biomass and functional community structure parameters in organic co-contaminated groundwater via respiratory quinone profiling

Moye Luo
Nanjing Institute of Environmental Sciences
Lixiang Zhu
Southeast University
Xin Zhu
Nanjing Institute of Environmental Sciences
Qinjun Liang
Southeast University
Tao Long
Nanjing Institute of Environmental Sciences
Manjun Zhan
Nanjing Environmental Protection Bureau
Xiaodong Zhang
Nanjing Institute of Environmental Sciences
Ran Yu
yuran@seu.edu.cn

Southeast University

Article

Keywords: respiratory quinone, microbial biomass, co-contaminated groundwater, bioremediation, parameter estimation

Posted Date: July 1st, 2026

DOI: https://doi.org/10.21203/rs.3.rs-9881973/v1

License: This work is licensed under a Creative Commons Attribution 4.0 International License.
Read Full License

Additional Declarations: No competing interests reported.

TITLE PAGE

Model-based estimation of microbial biomass and functional community structure parameters in organic co-contaminated groundwater via respiratory quinone profiling

Moye Luo [1,2], Lixiang Zhu [1,2], Xin Zhu [1], Qinjun Liang [1,2], Tao Long [1], Manjun Zhan [3], Xiaodong Zhang [1*], Ran Yu [2*]

[1] State Environmental Protection Key Laboratory of Soil Environmental Management and Pollution Control, Nanjing Institute of Environmental Sciences, MEE, Nanjing, Jiangsu, China 210042

[2] Department of Environmental Science and Engineering, School of Energy and Environment, Southeast University, Nanjing, Jiangsu, China 210096

[3] Nanjing Research Institute of Environmental Protection, Nanjing Environmental Protection Bureau, Nanjing, Jiangsu 210013, China

*** Corresponding author:**

Xiaodong Zhang, State Environmental Protection Key Laboratory of Soil Environmental Management and Pollution Control, Nanjing Institute of Environmental Sciences, Ministry of Ecology and Environment of China, Nanjing, 210042, China; email: Xiaodong Zhang@nies.org

Ran Yu, Department of Environmental Science and Engineering, School of Energy and Environment, Southeast University, No.2 Sipailou Street, Nanjing, 210096, China; Phone: (+86) 15312083786; Fax: (+86) 25 83792614; email: yuran@seu.edu.cn

Abstract

Effective numerical modeling of *in situ* bioremediation requires high-frequency tracking and real-time feedback of microbial community dynamics for parameter adjustment. However, traditional microbial characterization methods are time-intensive and poorly suited for field deployment, limiting the dynamic simulation of bioremediation processes. Respiratory quinones (RQs) are lipid-soluble molecules involved in microbial electron transport and serve as taxon-specific biomarkers for microbial community characterization. This study evaluated the feasibility of using RQs as chemical biomarkers to quantify microbial biomass and functional community structure in groundwater co-contaminated with BTEX and chlorinated ethenes. The correlation of quinone profiles with biomass and community structure of different microbial groups was explored, and quantitative RQ-microbial populations indication models were further developed. The results showed that each of the four functionally distinct microbial populations, categorized by degradation capability and oxygen requirement, exhibited strong correlations with key quinone types. A significant linear relationship was also observed between total quinone content and microbial biomass carbon ($R^2 = 0.85$), enabling quantitative estimation of total biomass. Multiple linear regression models demonstrated robust performance ($R^2 > 0.626$), with optimized predictor sets requiring only 3–4 RQ variables. This study highlighted the potential of using RQs as the convenient candidate indicator for rapid and field-applicable microbial assessment and evaluated their suitability for *in situ* bioremediation models.

Keywords: respiratory quinone, microbial biomass, co-contaminated groundwater, bioremediation, parameter estimation

1 Introduction

Groundwater ecosystems are intricate and host diverse microbial communities that play essential roles in contaminant degradation. Biodegradation—either natural or engineered—is a pivotal aspect of groundwater remediation strategies [1,2]. The effectiveness of microbial degradation depends not only on biomass but also on the structure and functions of microbial communities [3,4]. Reactive transport models have emerged as a valuable and indispensable tool for understanding and predicting the fate of organic contaminants during biodegradation [5]. They are widely used for encompassing fundamental investigations into the underlying mechanisms governing the transport and fate of organic contaminant plumes, as well as the practical aspects of plume management and the design of remediation systems [6]. However, a key limitation of such models lies in the challenge of rapidly and accurately quantifying microbial biomass and community structure in a field-applicable manner [7]—parameters that are essential for simulating biodegradation in subsurface environments.

On-line monitoring technologies are increasingly integrated into groundwater management practices. They enable continuous and comprehensive monitoring of contaminated groundwater, supporting the development of robust datasets for numerical modeling [8,9]. Reactive transport modeling for *in situ* bioremediation requires more than monitoring of physical and chemical parameters (e.g. environmental conditions and contaminant depletion), they also demand temporal tracking of microbial community dynamics to inform model calibration in real time. However,

current sensor technologies lack the capability to provide real-time, quantitative measurements of microbial biomass and community composition directly in subsurface environments, thereby limiting the application of the technology into bioremediation modeling frameworks.

Respiratory quinones (RQs) are lipid-soluble molecules involved in microbial electron transport and serve as taxon-specific biomarkers for microbial community characterization in aquifer systems [10,11]. Respiratory quinone profiling offers a practical approach to infer microbial traits (biomass and community structure) that are otherwise difficult to measure directly, by translating them into chemically quantifiable indicators suitable for field detection [12]. These indicators can then be integrated into numerical models to estimate microbial parameters relevant to biodegradation kinetics. As such, respiratory quinone profiling holds strong potential for integration into real-time microbial monitoring systems in groundwater remediation.

The primary RQs serving as biomarkers are ubiquinone (UQ) and menaquinone (MK), which function as electron carriers in microbial respiratory chains and exhibit strong taxonomic specificity. Total quinone content (TQ)—defined as the sum of all detectable quinone species—has demonstrated a linear relationship with microbial biomass in systems [13,14]. This supports its application as a proxy indicator of biomass fluctuations in groundwater settings. Quinone synthesis is closely linked to microbial phylogeny and electron transport requirements. Most microorganisms produce a single dominant quinone type, allowing quinone profiles to reflect community composition

87 and function [15]. Respiratory quinone profiling holds promise for characterizing the
88 structural features of microbial communities by quantifying the total content, type, and
89 relative abundance of quinone species in environmental samples.

90 Several studies have investigated the application of respiratory quinone profile to
91 assess microbial biomass and community composition. Early work by Collins and Jones
92 [16] highlighted the value of quinone composition in microbial taxonomy. They
93 demonstrated that quinone structures vary systematically among taxa, providing useful
94 chemotaxonomic markers. Fujie et al. [17] confirmed this potential by correlating quinone
95 abundance with microbial community diversity in soil samples. However, these studies
96 remained qualitative and lacked a framework for quantitatively linking quinone
97 composition to microbial parameters. In terms of correlating quinone with microbial
98 activity, Becker et al. [18] used quinone profiling to explore redox processes and microbial
99 diversity in Black Sea sediments. They demonstrated that shifts in quinone composition
100 reliably reflected heterotrophic microbial activity under different redox conditions.
101 Collectively, these studies have established qualitative links between quinone profiles
102 and microbial structure, yet few have quantitatively defined these relationships in a
103 modeling context. In particular, applications of quinone biomarkers to parameterize
104 biodegradation models in groundwater remain rare.

105 In this study, the quantitative relationship between respiratory quinone profiles and
106 microbial community dynamics in contaminated groundwater was investigated to
107 provide parameter estimation methods for our previously developed multi-level

substrate interaction model (MSIM) [19]. Perchloroethylene (PCE) and benzene, which are common groundwater contaminants, were used as target species. The laboratory-scale microcosms under five scenarios were established to analyze the relationship between RQ composition and microbial community dynamics, including natural attenuation, biostimulation, bioaugmentation, and co-contamination with PCE and benzene at both low and high concentrations. The association between total quinone content (TQ) and microbial biomass, expressed as microbial total organic carbon (MTOC), was evaluated. The links between specific quinone species and microbial communities at both phylum and genus levels, as well as four microbial functional groups, were investigated by two-matrix correlation analyses. The microbial functional groups were defined based on the parameters in the degradation model as: (i) aerobic benzene degraders, $X_{B,\,Aer}$, (ii) aerobic PCE & benzene co-degraders, $X_{B\&C,\,Aer}$, (iii) anaerobic PCE degraders, $X_{C,\,An}$, and (iv) anaerobic PCE & benzene co-degraders, $X_{B\&C,\,An}$. Finally, regression models were developed to estimate the abundance of these microbial groups from quinone profiles, providing key biological parameters for integration into the MSIM.

2 Materials and methods

2.1 Field sampling

The soil cores and groundwater samples used in this study were collected from a closed pesticide plant in Jiangsu province, China. The site was contaminated with PCE and benzene, toluene, ethylbenzene, and xylene (BTEX). The soil samples were

129 collected using a Direct Push Drilling Rig (6712DT, Geoprobe, USA) from 6 to 9 m
130 below ground, which is the primary contamination zone. Groundwater samples were
131 collected with the bailers from the monitoring wells near the soil sampling sites. All the
132 samples were kept on dry ice during transport and stored at -80℃ upon arrival at the
133 laboratory. All necessary permissions and permits for sample collection were formally
134 obtained from the relevant local authorities and the site management. Furthermore,
135 research data from this study site have been successfully utilized in previously peer-
136 reviewed publications [20].

137 **2.2 Microcosm experimental setup**

138 The microcosm systems were constructed in 40 ml amber volatile organic analysis
139 (VOA) bottles with spiral caps and polytetrafluoroethylene (PTFE) septa. Each bottle
140 was filled with a homogenized slurry prepared by combining groundwater and
141 contaminated soil collected from the study site. The microcosms were incubated in the
142 dark on a rotary shaker maintained at 8 rpm to ensure continuous mixing. At 180-day
143 intervals, three replicate bottles from each treatment group were collected for analysis
144 of respiratory quinones, microbial biomass, and microbial community composition,
145 following standardized sample pretreatment procedures. The total incubation period
146 was 360 days.

147 The experimental design included five treatment scenarios: (1) natural attenuation
148 (NA), (2) biostimulation (BS), (3) bioaugmentation (BA) under PCE-only conditions,
149 and two co-contamination scenarios involving PCE and benzene at different molar

ratios, (4) PCE+BZ_L (1:1 benzene to PCE) and (5) PCE+BZ_H (10:1 benzene to PCE). All microcosm setups were performed in independent biological triplicates to ensure the reproducibility and statistical reliability of the results. Sample codes corresponding to each treatment group and sampling time point were summarized in Table 1. The sterilized control group, in which neither quinones nor microorganisms were detected, was excluded from subsequent analyses.

2.3 Measurement of MTOC

The MTOC content was quantified using the chloroform fumigation-extraction method, as originally described by Vance et al. [21]. This method is a widely accepted technique for measuring microbial biomass in the solid phase. In groundwater systems, more than 99% of microbial biomass is typically associated with the solid matrix rather than the aqueous phase [22]. Briefly, the procedure involves three main steps: fumigation, extraction, and quantification. Fresh soil samples were fumigated with chloroform for 24 hours to lyse microbial cells and release intracellular carbon. Following fumigation, microbial carbon was extracted using 0.5 mol/L K_2SO_4 solution. The extractable organic carbon was then measured using a TOC analyzer (Model 1030, Aurora O.I. Analytical, USA) to determine the MTOC content.

2.4 Extraction and analysis of quinones

A 10 g air-dried soil was mixed with 40 mL of a 2:1 (v/v) chloroform–methanol solution. The mixture was shaken for 10 minutes and then ultrasonically treated for 10 minutes at 20 kHz and 100-120 W. Following centrifugation at 10000 × g for 10 minutes

171 to separate the lipid layer, which was collected as the supernatant. This procedure was
172 repeated three times. The extracts were combined, filtered through a 0.45 μm membrane,
173 and concentrated by drying at 40°C. Subsequently, 5 mL of a saline solution (containing
174 1 g/L $CaCl_2$ and 10 g/L NaCl) and 25 mL of n-hexane were added to the concentrate.
175 After 10 minutes of shaking, the liquid–liquid extraction was performed twice. The
176 extract was concentrated to 5 mL and then passed through two Sep-Pak Silica columns
177 (WAT020810, Waters, USA) connected in series. MKs were eluted with 10 mL of a
178 2:98 (v/v) diethyl ether–n-hexane mixture, and UQs were eluted with 10 mL of a 10:90
179 (v/v) diethyl ether–n-hexane mixture. The concentrated extracts were evaporated to
180 dryness under a gentle stream of nitrogen, re-dissolved in acetone, and analyzed using
181 a high-performance liquid chromatography system (HPLC, 1260 Infinity II, Agilent
182 Technologies, USA) equipped with a photodiode array detector.

183 MK-7 and UQ-10 were used as standards for quantification, and quinone contents
184 were calibrated based on the maximum absorbance peak determined by full-wavelength
185 scanning. Optimal chromatographic conditions were determined by analyzing the peak
186 area and standard curve linearity. Previous studies have shown that the mobile phase
187 type has a limited effect on UQs and MKs detection, with a negligible impact on
188 standard curve fit under various conditions [17]. Therefore, isopropanol was selected as
189 the mobile phase, as it is considered more cost-effective and environmentally preferable
190 than isopropyl ether. The detailed operating conditions for the quantification of
191 respiratory quinones by HPLC were provided in Table S1.

2.5 DNA extraction and polymerase chain reaction (PCR) Amplification

Genomic DNA was extracted from the solid phase of centrifuged microcosm slurry using the Mag-bind Soil DNA Extraction Kit (E.Z.N.A., OMEGA, USA). The V3-V4 region of bacterial 16S rRNA gene was amplified with primers 341f (5'-CCCTACACACGACGCTCTTCCGATCTG-3') and 806r (5'-GGACTACNNGGGTATCTAAT-3'). Paired-end sequencing (2 × 250 bp) was performed on an Illumina MiSeq platform (Sangon Biotech, Shanghai, China). Detailed protocols for DNA extraction, PCR amplification, read quality control, OTU clustering, and taxonomic annotation were provided in Supplementary Material 1.

2.6 Data analysis

TQ was used as an indicator for quantifying microbial biomass. The equation for calculation TQ is presented as follows:

$$TQ = \sum_{k=1}^{n} C_k \tag{2.1}$$

Where C_k is the molar or mass concentration of quinone k (μmol·kg^{-1}), and n is the number of quinone species.

Statistical indices of disparity and diversity were employed to analyze the relationship between quinone diversity and microbial community diversity. The disparity index (D) was calculated based on the method described by Hiraishi et al. [23], as follows:

$$D(i, j) = 1/2 \sum_{k=1}^{n} \left| P_{ki} - P_{kj} \right| \times 100 \tag{2.2}$$

Where P_{ki} and P_{kj} represent the molar fractions of the k-th quinone component in

211 samples *i* and *j*, respectively. The disparity index is expressed as a percentage.

212 The quinone diversity index (DQ) was calculated according to Hu et al. [24]as

213 follows:

$$DQ = \left(\sum_{k=1}^{n} \sqrt{P_k} \right)^2 \quad (2.3)$$

214 Where P_k represents the molar proportion of the *k*-th quinone component and *n* is

215 the total number of quinone types.

216 Experimental data was utilized to evaluate fluctuations in the extracted quinone

217 amounts and the disparity index of the quinone profiles. Cumulative frequencies for

218 quinone diversity and disparity were determined based on variations in replicate

219 measurements, assuming a normal distribution for extraction differences and a log-

220 normal distribution for disparity differences.

221 The Mean Absolute Error (MAE) and Mean Absolute Percentage Error (MAPE)

222 were employed as metrics to evaluate prediction accuracy. The expressions for these

223 error evaluation metrics were provided in equations (2.4) and (2.5).

$$\mathrm{MAE}=\frac{1}{n}\sum_{i=1}^{n}|y_i-\widehat{y_i}| \quad (2.4)$$

$$\mathrm{MAPE}=\frac{1}{n}\sum_{i=1}^{n}\left|\frac{y_i-\widehat{y_i}}{yi}\right| \quad (2.5)$$

224 Where:

225 y_i is the observed value, $\widehat{y_i}$ is the predicted value, $\overline{y_i}$ is the average of the

226 observed values, *n* is the number of data points.

227 The multiple linear regression (MLR) approach was applied to establish a

228 relationship model between quinone profiles and microbial populations. Although more

complex models may yield higher R^2, the multiple linear regression was selected for its parsimony. It reduces overfitting under limited and noisy microcosm data while offering transparent, computationally efficient formulations for integration into the MSIM. The analysis was conducted using IBM SPSS Statistics 26.0 software, which provided regression coefficients, interval estimates, residuals with confidence intervals, and model status parameters, including the coefficient of determination (R^2), F-value with its significance, and estimated error variance. The basic multiple linear regression equation is as follows:

$$y = \beta_0 + \beta_1 x_1 + \beta_2 x_2 + ... + \beta_p x_p + \varepsilon \qquad \varepsilon \sim N(0, \sigma^2) \tag{2.6}$$

Where:

x_i represents the observed values of the independent variables, y represents the predicted value from the nonlinear regression, ε represents the residual between the predicted and actual values of the dependent variable.

To optimize the predictor selection and ensure model stability, a stepwise regression method was employed. Furthermore, collinearity diagnostics were performed to evaluate potential multicollinearity among the independent variables. The Variance Inflation Factor (VIF) was calculated, with a widely accepted threshold of VIF < 10 indicating the absence of severe multicollinearity.

2.7 Statistical analysis

Student's T-test and Pearson correlation analysis were employed to assess the significance of differences between two groups. For comparisons involving more than

two groups, the Kruskal-Wallis H test was used to evaluate inter-group differences. A p-value of $\leq$ 0.05 was considered statistically significant.

3 Results

3.1 Characteristics of respiratory quinone profiles

Under varying contamination scenarios, TQ levels in the microcosm systems consistently increased over time, with significantly higher growth rates observed in the BA and PCE+BZ_L groups, as shown in Fig. S1 in the Supplementary Information (SI). In the single-contaminant groups, TQ levels in the BA and BS groups increased by $58.06 \pm 2.34\%$ and $51.24 \pm 6.15\%$, respectively, compared to the NA group, indicating that enhanced attenuation strategies promoted microbial biomass accumulation. The most rapid increase in TQ occurred during the early stage of the experiment, with the BA and NA groups reaching 98.66% and 99.76% of their final values by day 180, suggesting a stabilization of microbial biomass during the later phase of incubation. In the co-contamination systems, peak TQ levels were generally higher than those observed under single-contaminant conditions, implying that the presence of benzene further stimulated microbial growth. However, in PCE+BZ_H group, a rise-then-decline pattern in TQ level was observed, which is likely attributable to oxygen depletion that led to inactivation of benzene-degrading microorganisms previously active under aerobic conditions.

Quinone profiles were constructed based on the relative abundance of various respiratory quinones, as shown in Fig. S2 in the SI. At the beginning of the experiment,

MK-11 dominated all groups but steadily declined over time, while UQ-8 and UQ-9 increased consistently. In the single-contaminant groups, MK-9 (H_2) dominated the BA group during the early phase (50.19 ± 1.64%). However, UQ-type quinones gradually replaced it as the dominant quinone, likely reflecting a microbial succession process where the initially inoculated community was overtaken by active degraders under selective pressure. In the BS group, UQ-9 remained the dominant quinone throughout, suggesting a strong association with PCE-degrading microorganisms. In the co-contamination groups, UQ-8 and MK-8(H_2) were significantly enriched ($p < 0.05$), indicating their potential involvement in BTEX degradation. Additionally, UQ-9 abundance was markedly higher in the PCE+BZ_L group than in other scenarios, reinforcing its role in PCE biodegradation.

Respiratory quinone diversity was generally higher in the co-contamination groups than in the single-contaminant scenarios, as shown in Table. S2 in the SI. The BS group exhibited the highest quinone diversity, likely due to the introduction of substrates and electron donors [25]. Quinone community dissimilarity analysis revealed significant variations in quinone composition across most experimental group and time points. Minor differences were observed between the BS and co-contamination groups at the initial stage ($D(i, j) < 10$), but substantial divergence was detected both across groups and over time within the same group ($D(i, j) > 10$), as shown in Table. S3 in the SI. These results highlight the sensitivity and potential of respiratory quinone profiling as a dynamic indicator of microbial community responses under

291 contamination stress.

292 **3.2 Microbial community composition and diversity**

293 MTOC levels closely followed the trend of TQ, with a strong positive correlation
294 observed (Pearson's r = 0.9953; as shown in Fig. S3 in the SI). This suggested
295 significant potential for establishing a quantitative relationship between the two
296 indicators. In the single- contaminant groups, MTOC levels in the BA and BS groups
297 increased by 23.54 ± 1.19% and 29.72 ± 3.01%, respectively, compared to the NA group.
298 Notably, MTOC levels were higher in co-contaminated groups, although a decline was
299 observed on day 360.

300 Approximately 999,400 high-quality 16S rRNA sequences were obtained from 30
301 microcosm samples, with an average coverage of 97.2 ± 1.7%. These sequences were
302 clustered into 2,658 OTUs, spanning 47 phyla and 852 genera. At the phylum level,
303 Proteobacteria dominated across all groups, followed by Firmicutes, Actinobacteriota,
304 and Bacteroidota (Fig. 1a). In the co-contamination scenarios, Proteobacteria
305 consistently represented more than 45% of the microbial community. In the
306 PCE+BZ_H group, Actinobacteriota decreased significantly from 38.96% on day 180
307 to 8.42% on day 360. Bacteroidota remained relatively stable in the co-contamination
308 groups (5.05%–9.68%) but they were seldom detected in the single-contaminant
309 scenarios. At the genus level, *Pseudomonas*, *Ralstonia*, and *Arthrobacter* were
310 predominant in single-contaminant microcosms. *Pseudomonas* showed the highest
311 relative abundance in the BA group, while the NA group exhibited a more diverse genus

312 distribution (Fig. 1b). Co-contamination significantly altered the dominant genera:
313 *Pseudoxanthomonas* increased steadily in the PCE+BZ_L group, whereas *Ralstonia*
314 became dominant in the later stages in the PCE+BZ_H group. These shifts suggested
315 that the presence of benzene may be a key driver of microbial community succession.
316 At the phylum level, Proteobacteria consistently emerging as the dominant phylum
317 in all groups, whereas at the genus level, substantial differences were observed between
318 single-contaminant and co-contaminant systems (Fig. 2). In single-contaminant
319 microcosms, *Pseudomonas* was the predominant genus. In contrast, co-contamination
320 led to more pronounced genus-level shifts: *Pseudoxanthomonas* and *Ralstonia*
321 dominated under low and high benzene concentrations, respectively, while
322 *Pseudomonas* played a secondary role. These findings underscore the critical role of
323 benzene as a selective factor driving microbial community succession. On the other
324 hand, the low taxonomic overlap between contamination groups suggested that each
325 scenario shaped a highly specific microbial community structure, as shown in Fig. S4
326 and Table S4. Of the 2,658 OTUs identified, only 287 (10.80%) were shared among all
327 five groups. The BA and PCE+BZ_H group exhibited the highest numbers of unique
328 OTUs, accounting for 11.51% and 10.23% of the total, respectively. In contrast, OTU
329 overlap among any two to four contamination groups was markedly lower, comprising
330 less than 5% of the total OTUs. In summary, the distinct microbial successions driven
331 by various co-contamination scenarios highlight the necessity of identifying stable
332 chemical biomarkers, thereby enabling a subsequent quantitative assessment that links

these specific functional groups with RQ profiles.

3.3 Correlation analysis between quinone profile and microbial community

A strong linear correlation was observed between TQ and MTOC in the microcosm systems (Fig. 3). The linear regression equation was established as follows:

$$C_{MTOC} = 8.962 \times C_{TQ} + 28.15,$$

The model yielded a coefficient of determination ($R^2 = 0.85$, $p < 0.05$), indicating a strong positive relationship between TQ and microbial biomass. These results suggested that the TQ-MTOC regression model can serve as a promising tool for estimating microbial abundance in groundwater systems using chemical indicators.

At both phylum and genus levels, the quinone composition exhibited significant correlations with the certain microbial community, as determined by Pearson correlation analysis ($P < 0.05$). However, the phylum-level correlations were predominantly negative, whereas genus-level associations frequently exhibited a many-to-one pattern, with multiple microbial genera correlating with individual quinone type (Fig. 4). At the phylum level, MK-11 showed significant positive correlations with Acidobacteriota, Verrucomicrobiota, Bdellovibrionota, and PCP2-54, whereas UQ-9 and MK-8(H_2) were positively associated with GAL15 ($p < 0.05$). Since respiratory quinones serve as electron carriers in the microbial electron transport chains, their abundance is theoretically expected to positively correlate with microbial community dynamics [26]. Therefore, microbial phyla exhibiting negative correlations with quinone profiles were excluded from further analysis. At the genus level, UQ-6, UQ-8, UQ-9,

and MK-6 were positively correlated with *Pseudoxanthomonas*, while UQ-7 and MK-10 showed strong associations with *Desulfurispora* and *unclassified_f_Enterobacteriaceae*, respectively. Nevertheless, these genus-level correlations were relatively sparse and exhibited inconsistent patterns, suggesting that quinone profiles alone may be insufficient for precise characterization of microbial composition at finer taxonomic levels.

The genus-level microbial communities identified through sequencing were functionally classified based on their documented capacities to degrade BTEX and highly chlorinated ethenes (CEs), as well as their oxygen requirements (Table 2). This classification enabled subsequent correlation analysis between functional microbial groups and respiratory quinone composition (Fig. 5). Among the twenty most abundant genera across the five microcosms, ten genera exhibited known BTEX-degrading capabilities, including well-characterized taxa such as *Pseudomonas*, *Ralstonia*, and *Rhodococcus*. Of these, seven were aerobic BTEX degraders, while three were anaerobic taxa typically involved in co-metabolic processes. Additionally, eight dominant genera demonstrated the ability to degrade CEs, with *Ralstonia*, *Rhodoferax*, and *Rhodococcus* being the most prominen. Six of these were aerobic degraders, mainly associated with co-metabolic degradation pathways, whereas two were obligatory anaerobes. Notably, classical anaerobic reductive dechlorinators such as *Dehalobacter*, *Geobacter*, and *Dehalococcoides* were not dominant in any of the tested microcosms.

Based on documented degradation capabilities and oxygen requirements, the

375 microbial community was further categorized into four functional groups
376 corresponding to the microbiological input parameters of the MSIM model (Table 3):
377 (i) aerobic BTEX degraders ($X_{B,Aer}$), (ii) aerobic BTEX & CEs co-degraders ($X_{B\&C,Aer}$),
378 (iii) anaerobic CEs degraders ($X_{C,An}$), and (iv) anaerobic BTEX & CEs co-degraders
379 ($X_{B\&C,An}$). The relative abundance of each functional group was estimated by summing
380 the abundances of the corresponding genera. Due to the broad functional and ecological
381 diversity encompassed within phylum-level taxonomic classifications, which often
382 span multiple substrate degradation pathways and oxygen affinities, phylum-level
383 groupings excluded from functional analysis in this study. In the other hand, although
384 anaerobic functional degraders may not be numerically dominant in the bulk
385 community, their inclusion in the model is indispensable, as they drive the reductive
386 dechlorination of CEs, which is a critical biogeochemical function during the inevitable
387 transition to anaerobic conditions in mixed-plume aquifers.

388 Correlation analysis revealed significant associations between the four
389 functionally defined microbial groups and respiratory quinone composition, with UQ-
390 6, UQ-8, MK-7, and MK-7(H_2) exhibiting the strongest correlations (Pearson's $r > 0.80$,
391 $p < 0.05$; Fig. 5). Under aerobic conditions, MK-7 showed a strong positive correlation
392 with $X_{B,Aer}$, while MK-9 and MK-6 exhibited moderate correlations. For $X_{B\&C,Aer}$, MK-
393 7(H_2) demonstrated a strong correlation, followed by MK-8 and MK-9. These quinones
394 were predominantly methylated naphthoquinones, consistent with findings by Zhu et
395 al. [27], which identified these compounds as characteristic biomarkers in benzene and

toluene degradation. Under anaerobic conditions, UQ-8 showed a significant negative correlation with $X_{C,An}$, whereas MK-9 and MK-7 were positively correlated. Additionally, UQ-6 exhibited a strong positive correlation with $X_{B\&C,An}$, with UQ-8 also displaying substantial correlation. These observations suggested that UQs may serve as potential biomarkers for anaerobic degradation pathways. Supporting evidence from Zhu et al. [15] similarly linked UQ-6 and UQ-8 to microbial degradation activity in trichloroethylene-contaminated soils. In summary, the observed significant correlations between specific quinone species and functionally microbial groups suggested that the diagnostic potential of quinone profiles for assessing microbial function under co-contaminated conditions. These findings provided a robust foundation for further quantitative modeling of microbial functional dynamics using quinone-based biomarkers. Having established strong pairwise correlations between specific RQs and functional microbial groups, the next step is to integrate these robust biomarkers into a predictive mathematical framework to quantitatively estimate microbial parameters.

3.4 Quantitative estimation of microbiological parameters using quinone profiles

The models developed to estimate the relative abundances of the functionally defined microbial populations demonstrated satisfactory performance in terms of both goodness-of-fit and statistical significance (Table 4). Predictor variables were selected as quinones whose relative abundances were positive correlations with the respective microbial groups ($r > 0.4$). The coefficient of determination (R^2) for all models greater than 0.5, with the lowest value being 0.626 for the $X_{B\&C,Aer}$ model, indicating that this

model explained 62.6% of the observed variance, which meeting the generally accepted threshold for model adequacy ($R^2 > 0.5$). Furthermore, F-tests for all models yielded p-values below 0.05, confirming their overall statistical significance. Notably, even the model with the lowest F-statistic ($F = 1.615$) met the significance criterion, suggesting that the relative abundances of key quinones were effective predictors of microbial community structure. The Durbin–Watson (D-W) statistics for all models fell within the acceptable range (0–4), indicating no significant autocorrelation in the residuals and supporting the independence and reliability of the model inputs. In addition, the VIF for all selected quinone variables in the optimized models remained strictly below 10, which justifies the exclusion of multicollinearity, demonstrating that the specific quinones contribute uniquely to the variance of the microbial populations, thereby ensuring the mathematical stability of the proposed models. Detailed modeling procedures and evaluation criteria were provided in Supplementary Material 2.

Furthermore, the absolute abundances of functional microbial communities were estimated using the microbiological parameter framework of the MSIM model. According to this framework, the absolute abundance of each microbial group was calculated by multiplying its relative abundance with the MTOC in the system:

$$X_{B,\,Aer} = C_{MTOC} \times \overline{X}_{B,\,Aer} \tag{5.5}$$

$$X_{B\&C,\,Aer} = C_{MTOC} \times \overline{X}_{B\&C,\,Aer} \tag{5.6}$$

$$X_{C,\,An} = C_{MTOC} \times \overline{X}_{C,\,An} \tag{5.7}$$

$$X_{B\&C,\,An} = C_{MTOC} \times \overline{X}_{B\&C,\,An} \tag{5.8}$$

Where:

$X_{B,\,Aer}$: absolute abundance of aerobic BTEX degraders (mg/kg).

$X_{B\&C,\,Aer}$: absolute abundance of aerobic BTEX & CEs co-degraders (mg/kg).

$X_{C,\,An}$: absolute abundance of anaerobic CEs degraders (mg/kg).

$X_{B\&C,\,An}$: absolute abundance of anaerobic BTEX & CEs co-degraders (mg/kg).

C_{MTOC}: total microbial carbon content in the aquifer matrix (mg/kg).

$\bar{X}$: relative abundance of the corresponding functional microbial group.

4 Discussion

The results presented above systematically demonstrate the feasibility of using RQs as quantitative proxies for both total microbial biomass and specific functional groups. The underlying biochemical mechanisms driving these quinone-microbe correlations were further explored, and their implications for field-scale bioremediation modeling were evaluated. Significant differences in both RQ profiles and microbial community compositions were observed across microcosms subjected to different contamination scenarios, as shown in Fig. S1. Notably, a statistically significant correlation ($p < 0.05$) was identified between quinone profiles and functionally classified microbial communities (Fig. 5). Compared to the single-contaminant scenario, the relative abundance of ubiquinone species (UQ-X) increased substantially under co-contamination (24.06% vs. 55.44%), along with a marked rise in the quinone diversity index, as shown in Table. S2. These shifts in quinone composition and diversity are likely attributable to changes in substrate bioavailability and microbial

succession dynamics driven by the coexistence of multiple contaminants [28,29].

The presence of diverse contaminants may expand the range of available substrates and microbial metabolic pathways, thereby promoting greater quinone diversity. According to Wang et al. [11], UQ-X serve as biomarkers for α-, β-, and γ-Proteobacteria, as well as certain fungal taxa. Among these, UQ-8 was the predominant quinone detected across all co-contaminated samples (ranging from 13.34% to 26.82%), indicating a potential predominance of β-Proteobacteria under such conditions [30]. This bacterial class includes numerous aerobic, facultative anaerobic, and chemotrophic species capable of degrading various organic contaminants [31]. Notably, genera such as *Ralstonia* and *Rhodoferax* are likely key contributors to the biodegradation of BTEX and CEs under co-contaminated conditions, based on their well-documented metabolic capacities. From a metabolic standpoint, microorganisms rely on redox reactions to drive transmembrane electron transport, which in turn fuels ATP synthesis [10,32,33]. As integral components of the electron transport chain, respiratory quinones directly participate in these processes. Therefore, the observed increase in quinone diversity under co-contamination conditions likely reflects the enhanced complexity and functional redundancy of microbial energy metabolism. These findings provide mechanistic evidence supporting the use of quinone profiles as functional indicators of microbial responses in complex contamination scenarios. Rather than re-validating the fundamental biochemical roles of these quinones - which have been extensively documented in foundational microbiological studies [10,12] - this study strategically

476 leverages their established functional specificities to develop a macroscopic,
477 engineering-oriented proxy.

478 The strong correlation observed between respiratory quinone profiles and
479 functional microbial communities (Table 5, $R > 0.8$) likely arises from the biochemical
480 specificity of quinone biosynthesis. This process is governed not only by the
481 phylogenetic affiliation of microorganisms but also by the redox potential requirements
482 of their electron transport chains (ETC) [34]. Consequently, microbial populations with
483 similar metabolic functions tend to synthesize the same types of respiratory quinones
484 [16]. This biochemical specificity enhances the functional resolution of quinone profiling,
485 making it more effective than traditional taxonomic classification for characterizing
486 functional microbial community. Similar patterns have been reported in petroleum
487 hydrocarbon [7,17] and pentachlorophenol-contaminated soils [35], where changes in
488 quinone composition closely reflected contaminant degradation dynamics and
489 stabilized following contaminant removal. These results support the use of quinone
490 profiling as a rapid, sensitive and sustainable tool for monitoring functional shifts in
491 microbial communities under contaminant-induced stress.

492 On the other hand, the significant correlations observed between specific quinone
493 species and functional microbial groups (e.g., UQ-8 with aerobic microorganisms and
494 MK-7 with anaerobic microorganisms) may also arise from the distinct thermodynamic
495 properties of these biomolecules within the microbial ETC [36]. UQs possess a relatively
496 high midpoint redox potential (approximately +110 mV) and are predominantly

497 synthesized by strictly aerobic or facultatively anaerobic bacteria (such as
498 *Proteobacteria*) [10,37]. They are highly efficient in mediating electron transfer to high-
499 potential terminal electron acceptors, predominantly oxygen. This thermodynamic trait
500 explains the significant enrichment of UQ-6 and UQ-8 and their strong positive
501 correlations with aerobic BTEX and CEs co-degraders ($X_{B\&C,\ Aer}$) observed in our co-
502 contaminated microcosms. Conversely, MKs exhibit a significantly lower midpoint
503 redox potential (approximately -74 mV). This lower potential makes MKs
504 thermodynamically essential for coupling electron donors to lower-potential alternative
505 electron acceptors during anaerobic respiration [12,37], such as the reductive
506 dechlorination of CEs. Consequently, MK-7 and its variants serve as critical electron
507 carriers in anaerobic dehalorespiration pathways, inherently explaining their strong
508 correlation with anaerobic functional degraders ($X_{C,\ An}$ and $X_{B\&C,\ An}$). The
509 correspondence between these specific quinones and their obligatory thermodynamic
510 roles in the ETC reflects the mechanisms of the main terminal electron acceptance
511 processes and respiratory strategies adopted by microbial communities under co-
512 contaminant stress.

513 As essential components of the microbial electron transport chain, respiratory
514 quinones are likely synthesized in association with enzymatic systems responsible for
515 substrate metabolism. These molecules not only facilitate electron transfer and maintain
516 redox homeostasis, but also serve as informative taxonomic and functional biomarkers
517 in microbial ecology [38]. In this study, several specific quinone types exhibited strong

positive correlations with functionally defined microbial populations (Fig. 5, R > 0.8), and their abundance patterns aligned closely with the degradation capacities for target contaminants. These findings further confirm the functional indicative potential of quinone profiles. As noted by Marreiros et al. [39], quinones function as lipid-soluble electron carriers that bridge membrane-bound protein complexes and soluble enzymes within respiratory pathways. This mechanistic insight provides a new perspective for understanding the integrated "*microbe–enzyme–quinone*" response under contaminant-induced stress and reinforces the value of quinone profiling in evaluating functional shifts in microbial communities.

Numerical modeling of *in situ* bioremediation requires rapid, dynamic, and functionally relevant microbial input parameters, thereby imposing an urgent demand on real-time microbial monitoring techniques. However, the acquisition of such microbial parameters remains constrained by the limited availability of rapid and field-deployable detection technologies. To address this issue, this study proposed a quinone profiling approach as a functional proxy for microbial community structure. By identifying key quinone species that exhibit strong correlations with specific microbial groups, regression-based models were developed to enable rapid and quantitative estimation of microbial community composition. Compared to contemporary molecular techniques and bioinformatic functional prediction tools, the RQ-based proxies developed herein offer a distinct engineering trade-off. While multi-omics approaches provide unparalleled micro-scale resolution of functional gene networks, they are

frequently constrained by high analytical costs, extensive bioinformatic requirements, and complex data structures that are difficult to integrate directly into differential equation solvers [40,41]. Conversely, the proposed MLR models sacrifice deep ecological resolution in favor of macro-scale cost-effectiveness, rapid turnaround, and mathematical simplicity. This makes the quinone-based approach highly complementary to traditional molecular tools, serving specifically as a streamlined alternative tailored for the high-frequency parameterization demands of field-scale reactive transport models.

While this study successfully demonstrates the feasibility of using RQ profiles as macroscopic functional proxies, several inherent limitations must be acknowledged to guide future research. Admittedly, the functional classification in this study relies on literature-based taxonomic inference (Table 2) rather than direct experimental verification. However, this macroscopic estimation provides a necessary balance between microbiological resolution and engineering feasibility. It aligns perfectly with our primary objective: developing a rapid, field-applicable chemical proxy to parameterize numerical bioremediation models. Moreover, the regression models were evaluated without an independent external dataset, limiting the immediate assessment of their broader generalization. Nevertheless, robust internal metrics confirm their validity as a site-specific, proof-of-concept framework. In addition, it is important to emphasize that the quantitative 'quinone–microbial' models established in this study demonstrate strong predictive correlations rather than strict biological causality.

Nevertheless, for the practical purpose of parameterizing numerical bioremediation models, these robust correlative proxies provide sufficient and highly valuable engineering insights, while the definitive causal mechanisms remain a compelling subject for future pure-culture and multi-omics investigations.

The transition from laboratory microcosms to field-scale bioremediation is the ultimate objective of the proposed RQ-based framework. In practice, RQ profiling offers distinct engineering advantages over multi-omics sequencing by providing a rapid, cost-effective, and standardized tool to obtain macroscopic functional parameters. These proxies can directly parameterize reactive transport models (such as MSIM) to guide timely *in situ* remediation strategies. However, actual field applications face inherent challenges, including aquifer spatial heterogeneity, complex geochemical fluctuations, and matrix-dependent extraction efficiencies, which may perturb established "*microbe–quinone*" correlations. Therefore, future pilot-scale studies are warranted to calibrate these models against diverse site-specific conditions and standardize sampling protocols, ultimately unlocking their full engineering potential. Consequently, despite certain limitations, the use of RQ profiles as macroscopic functional proxies offers a practical and adaptive solution for the dynamic updating of microbial input parameters in numerical models and held promise for application in field-scale engineering and bioremediation management.

5 Conclusion

This study demonstrated the feasibility of using respiratory quinone profiling as a

rapid and informative approach for estimating microbial biomass and functional community structure in multi-solvent co-contaminated groundwater. A quantitative "quinone–microbial" model was developed to support parameter estimation for our previously developed biodegradation model frameworks. The results showed that the composition and diversity of quinones differed substantially across contamination scenarios, with the presence of BTEX compounds associated with increased genus-level heterogeneity and enhanced quinone profile complexity. A statistically significant linear relationship was observed between the TQ and MTOC ($R^2 = 0.85$, $p < 0.05$). At the functional group level, all four major degrader populations exhibited stable positive correlations with specific quinone types (e.g., UQ-6, UQ-8, MK-7, MK-7(H_2)). Compared to taxonomy-based models, the quinone profiling approach showed higher convenience and greater adaptability as a functional indicator. The regression model achieved statistical significance while optimizing the number of input variables, thereby improving both its applicability and computational efficiency. Overall, the proposed approach offered a promising solution for field-based microbial parameter quantification, especially in environments lacking microbial monitoring infrastructure.

Funding Statements

This work was supported by the National Key R&D Program of China [grant number 2024YFC3713304], National Key R&D Program of China [grant number 2023YFC3709600].

Author contributions

Moye Luo: Conceptualization; Methodology; Writing - original draft.

Lixiang Zhu: Validation.

Xin Zhu：Supervision.

Qinjun Liang: Data Curation.

Tao Long: Resources.

Manjun Zhan: Supervision.

Xiaodong Zhang: Writing - review & editing; Project administration.

Ran Yu: Writing - review & editing; Funding acquisition.

Data availability

The datasets generated and/or analyzed during the current study are available within the article and its Supplementary Information files. High-throughput sequencing data have been deposited in the NCBI Sequence Read Archive database with the accession number PRJNA703730.

Declaration of interests

The authors declare that they have no known competing financial interests or personal relationships that could have appeared to influence the work reported in this paper.

References

1 Stroo, H. F. *In Situ Remediation of Chlorinated Solvent Plumes*. (Springer Science+Business Media, LLC, 2010).

2 Zhang, X. *et al.* Field study of microbial community structure and dechlorination activity in a multi-solvents co-contaminated site undergoing natural attenuation. *Journal of Hazardous Materials* **423**, 127010 (2022). https://doi.org/https://doi.org/10.1016/j.jhazmat.2021.127010

3 Gomez, D. E., de Blanc, P. C., Rixey, W. G., Bedient, P. B. & Alvarez, P. J. J. Modeling benzene plume elongation mechanisms exerted by ethanol using RT3D with a general substrate interaction module. *Water Resources Research* **44** (2008). https://doi.org/10.1029/2007wr006184

4 Jin, D. *et al.* Diversity of bacteria and archaea in the groundwater contaminated by chlorinated solvents undergoing natural attenuation. *Environmental Research* **185** (2020). https://doi.org/10.1016/j.envres.2020.109457

5 Luo, M. *et al.* Bioremediation of chlorinated ethenes contaminated groundwater and the reactive transport modeling - A review. *Environmental research*, 117389 (2023). https://doi.org/10.1016/j.envres.2023.117389

6 Rifai, H. S., Borden, R. C., Newell, C. J. & Bedient, P. B. in *In Situ Remediation of Chlorinated Solvent Plumes* 145–184 (2010).

7 Song, D. J., Kitamura, M. & Katayama, A. Approach for Estimating Microbial Growth and Biodegradation of Hydrocarbon Contaminants in Subsoil Based on Field Measurements: 2. Application in a Field Lysimeter Experiment. *Environmental Science & Technology* **44**, 6795–6801 (2010). https://doi.org/10.1021/es100770g

8 Favere, J., Waegenaar, F., Boon, N. & De Gusseme, B. Online microbial monitoring of drinking water: How do different techniques respond to contaminations in practice? *Water Research* **202**, 117387 (2021).

9 Lyons, K. J. *et al.* Monitoring groundwater quality with real-time data, stable water isotopes, and microbial community analysis: A comparison with conventional methods. *Science of the Total Environment* **864**, 161199 (2023).

10 Abby, S. S., Kazemzadeh, K., Vragniau, C., Pelosi, L. & Pierrel, F. Advances in bacterial pathways for the biosynthesis of ubiquinone. *Biochimica et Biophysica Acta (BBA)-Bioenergetics* **1861**, 148259 (2020).

11 Wang, H., Wang, F. Y., Wei, Z. Q. & Hu, H. Y. Quinone profiles of microbial communities in sediments of Haihe River–Bohai Bay as influenced by heavy metals and environmental factors. *Environmental Monitoring and Assessment* **176**, 157–167 (2011).

12 Pelosi, L. *et al.* Ubiquinone Biosynthesis over the Entire O₂ Range: Characterization of a Conserved O₂-Independent Pathway. *mBio* **10**, 10.1128/mbio.01319–01319 (2019).

https://doi.org/doi:10.1128/mbio.01319-19

13 Hiraishi, A. *et al.* Significance of Lipoquinones as Quantitative Biomarkers of Bacterial Populations in the Environment. *Microbes and Environments* **18** (2003).

14 Saitou, K. *et al.* Linear relation between the amount of respiratory quinones and the microbial biomass in soil. *Soil Science and Plant Nutrition* **45** (1999).

15 Zhu, L., Luo, M., Zhang, X., Long, T. & Yu, R. Application of quinone profile method to indicate structure and activity of functional microbial community in trichloroethylene-contaminated soil. *CIESC Journal* **74(6)**, 2647–2654 (2023). https://doi.org/https://kns.cnki.net/kcms/detail/11.1946.TQ.20230524.1147.004.html

16 Collins, M. D. & Jones, D. Distribution of isoprenoid quinone structural types in bacteria and their taxonomic implication. *Microbiol Rev* **45**, 316–354 (1981).

17 Fujie, K. *et al.* Analysis of respiratory quinones in soil for characterization of microbiota. *Soil Science and Plant Nutrition* **44**, 393–404 (1998). https://doi.org/10.1080/00380768.1998.10414461

18 Becker, K. W. *et al.* Isoprenoid quinones resolve the stratification of redox processes in a biogeochemical continuum from the photic zone to deep anoxic sediments of the Black Sea. *Applied and Environmental Microbiology* **84**, e02736–02717 (2018).

19 Luo, M. *et al.* Modeling the elongation of commingled BTEX and chlorinated ethene plumes undergoing biodegradation with a multi-level substrate interaction module. *Journal of Hazardous Materials* **491** (2025). https://doi.org/10.1016/j.jhazmat.2025.137929

20 Zhang, X. *et al.* Field study of microbial community structure and dechlorination activity in a multi-solvents co-contaminated site undergoing natural attenuation. *J Hazard Mater* **423**, 127010 (2022). https://doi.org/10.1016/j.jhazmat.2021.127010

21 Vance, E. D., Brookes, P. C. & Jenkinson, D. S. An extraction method for measuring soil microbial biomass C. *Soil biology and Biochemistry* **19**, 703–707 (1987).

22 Lehman, R. M., Colwell, F. S. & Bala, G. A. Attached and unattached microbial communities in a simulated basalt aquifer under fracture-and porous-flow conditions. *Applied and Environmental Microbiology* **67**, 2799–2809 (2001).

23 Hiraishi, A., Morishima, Y. & Takeuchi, J. I. Numerical analysis of lipoquinone patterns in monitoring bacterial community dynamics in wastewater treatment systems. *J.gen.appl.microbiol* **37**, 57–70 (1991).

24 Hu, H. I. (Yokohama National University Yokohama, Japan,

1993).

25 Lyons, K. J. *et al.* Monitoring groundwater quality with real-time data, stable water isotopes, and microbial community analysis: A comparison with conventional methods. *Sci Total Environ* **864**, 161199 (2023). https://doi.org/10.1016/j.scitotenv.2022.161199

26 Hu, H. Y., Fujie, K., Nakagome, H., Urano, K. & Katayama, A. Quantitative analyses of the change in microbial diversity in a bioreactor for wastewater treatment based on respiratory quinones. *Water Research* **33**, 3263–3270 (1999).

27 Zhu, C. *Characterization of quinone fingerprints during biodegradation of typical organic pollutants at agrochemical contaminated sites.* master thesis, Southeast University, (2021).

28 Song, D. & Katayama, A. Monitoring microbial community in a subsurface soil contaminated with hydrocarbons by quinone profile. *Chemosphere* **59**, 305–314 (2005).

29 Kunihiro, T. *et al.* The succession of microbial community in the organic rich fish-farm sediment during bioremediation by introducing artificially mass-cultured colonies of a small polychaete, Capitella sp. I. *Marine pollution bulletin* **57**, 68–77 (2008).

30 Katayama, A., Funasaka, K. & Fujie, K. Changes in the respiratory quinone profile of a soil treated with pesticides. *Biology and Fertility of Soils* **33**, 454–459 (2001).

31 Chinalia, F. & Killham, K. S. 2, 4-Dichlorophenoxyacetic acid (2, 4-D) biodegradation in river sediments of Northeast-Scotland and its effect on the microbial communities (PLFA and DGGE). *Chemosphere* **64**, 1675–1683 (2006).

32 Hiraishi, A. Isoprenoid quinones as biomarkers of microbial populations in the environment. *Journal of Bioscience and Bioengineering* **88** (1999).

33 Hedrick, D. B. & White, D. C. Microbial respiratory quinones in the environment: I. A sensitive liquid chromatographic method. *Journal of microbiological methods* **5**, 243–254 (1986).

34 Nowicka, B. & Kruk, J. Occurrence, biosynthesis and function of isoprenoid quinones. *BBA - Bioenergetics* **1797** (2010).

35 Uchida, S., Tanaka, H., Fujie, K. & Katayama, A. Changes in microbial community structure in soil percolated with pentachlorophenol with reference to respiratory quinone profile. *Journal of Pesticide Science* **24**, 186–188 (1999).

36 Schoepp-Cothenet, B. *et al.* On the universal core of bioenergetics. *Biochimica et Biophysica Acta (BBA) - Bioenergetics* **1827**, 79–93 (2013). https://doi.org/https://doi.org/10.1016/j.bbabio.2012.09.005

37 Unden, G. & Bongaerts, J. Alternative respiratory pathways of

Escherichia coli: energetics and transcriptional regulation in response to electron acceptors. *Biochim Biophys Acta* **1320**, 217–234 (1997). https://doi.org/10.1016/s0005-2728(97)00034-0

38 Soballe, R. & Poolle, R. Microbial ubiquinones: multiple roles in respiration, gene regulation and oxidative stress management. *Microbiology-reading* **145**, 1817–1830 (1999).

39 Marreiros, B. C. *et al.* Exploring membrane respiratory chains. *Biochimica et Biophysica Acta (BBA)-Bioenergetics* **1857**, 1039–1067 (2016).

40 Thullner, M. & Regnier, P. Microbial Controls on the Biogeochemical Dynamics in the Subsurface. *Reviews in Mineralogy and Geochemistry* **85**, 265–302 (2019). https://doi.org/10.2138/rmg.2019.85.9

41 Song, H.-S. *et al.* Coupling flux balance analysis with reactive transport modeling through machine learning for rapid and stable simulation of microbial metabolic switching. *Scientific Reports* **15**, 6042 (2025). https://doi.org/10.1038/s41598-025-89997-9

42 Banerjee, S. *et al.* Isolation of Pseudomonas aromaticivorans sp. nov from a hydrocarbon-contaminated groundwater capable of degrading benzene-, toluene-, m- and p-xylene under microaerobic conditions. *Frontiers in Microbiology* **13** (2022). https://doi.org/10.3389/fmicb.2022.929128

43 Qiu, L. *et al.* Zinc and copper supplements enhance trichloroethylene removal by Pseudomonas plecoglossicida in water. *Environmental Technology* (2022). https://doi.org/10.1080/09593330.2022.2069518

44 Li, Y. *et al.* Aerobic co-metabolism of trichloroethylene using gasoline as primary substrate. *Chinese Journal of Environmental Engineering* **8**, 977–982 (2014).

45 Lee, S. K. & Lee, S. B. Isolation and characterization of a thermotolerant bacterium Ralstonia sp strain PHS1 that degrades benzene, toluene, ethylbenzene, and o-xylene. *Applied Microbiology and Biotechnology* **56**, 270–275 (2001). https://doi.org/10.1007/s002530100608

46 Kim, J. M. *et al.* Influence of Soil Components on the Biodegradation of Benzene, Toluene, Ethylbenzene, and o-, m-, and p-Xylenes by the Newly Isolated Bacterium Pseudoxanthomonas spadix BD-a59. *Applied and Environmental Microbiology* **74**, 7313–7320 (2008). https://doi.org/10.1128/aem.01695-08

47 Miri, S. *et al.* Evaluation of scale-up effect on cold-active enzyme production and biodegradation tests using pilot-scale bioreactors and a 3D soil tank. *Journal of Hazardous Materials* **450** (2023). https://doi.org/10.1016/j.jhazmat.2023.131078

48 Zhao, T. T. *et al.* Influence of methane and trichloroethylene domestication on bacterial community structure in landfill cover soil. *The journal of applied ecology* **28**, 1707–1715 (2017). https://doi.org/10.13287/j.1001-9332.201705.012

49 Huizenga, J. M. & Semprini, L. Influence of growth substrate and contaminant mixtures on the degradation of BTEX and MTBE by Rhodococcus rhodochrous ATCC strain 21198. *Biodegradation* (2023). https://doi.org/10.1007/s10532-023-10037-2

50 Suttinun, O., Mueller, R. & Luepromchai, E. Cometabolic Degradation of Trichloroethene by Rhodococcus sp Strain L4 Immobilized on Plant Materials Rich in Essential Oils. *Applied and Environmental Microbiology* **76**, 4684–4690 (2010). https://doi.org/10.1128/aem.03036-09

51 Wongbunmak, A., Khiawjan, S., Suphantharika, M. & Pongtharangkul, T. BTEX biodegradation by Bacillus amyloliquefaciens subsp. plantarum W1 and its proposed BTEX biodegradation pathways. *Scientific Reports* **10** (2020). https://doi.org/10.1038/s41598-020-74570-3

52 Kim, S., Bae, W., Hwang, J. & Park, J. Aerobic TCE degradation by encapsulated toluene-oxidizing bacteria, Pseudomonas putida and Bacillus spp. *Water Science and Technology* **62**, 1991–1997 (2010). https://doi.org/10.2166/wst.2010.471

53 Wu, Y. Q., Xu, Y. & Zhou, N. Y. A newly defined dioxygenase system from Mycobacterium vanbaalenii PYR-1 endowed with an enhanced activity of dihydroxylation of high-molecular-weight polyaromatic hydrocarbons. *Frontiers of Environmental Science & Engineering* **14** (2020). https://doi.org/10.1007/s11783-019-1193-5

54 Halsey, K. H., Sayavedra-Soto, L. A., Bottomley, P. J. & Arp, D. J. Trichloroethylene degradation by butane-oxidizing bacteria causes a spectrum of toxic effects. *Applied Microbiology and Biotechnology* **68**, 794–801 (2005). https://doi.org/10.1007/s00253-005-1944-z

55 Son, J., Lee, H., Kim, M., Kim, D. U. & Ka, J. O. Massilia aromaticivorans sp. nov., a BTEX Degrading Bacterium Isolated from Arctic Soil. *Current Microbiology* **78**, 2143–2150 (2021). https://doi.org/10.1007/s00284-021-02379-y

56 Mera, N. & Iwasaki, K. Use of plate-wash samples to monitor the fates of culturable bacteria in mercury- and trichloroethylene-contaminated soils. *Applied Microbiology and Biotechnology* **77**, 437–445 (2007). https://doi.org/10.1007/s00253-007-1152-0

57 Farkas, M. *et al.* Enrichment of dissimilatory Fe(III)-reducing bacteria from groundwater of the Sikls BTEX-contaminated site (Hungary). *Folia Microbiologica* **62**, 63–71 (2017). https://doi.org/10.1007/s12223-016-0473-8

58 Zaa, C. L. Y., McLean, J. E., Dupont, R. R., Norton, J. M. & Sorensen, D. L. Dechlorinating and iron reducing bacteria distribution in a TCE-contaminated aquifer. *Groundwater Monitoring & Remediation* **30**, 46–57 (2010).

Table Captions

Table 1 Microcosm experimental setup for quinone profile and microbial community analysis, and sample naming rules.

Table 2 List of functions and oxygen demand classification of microorganisms at genus level (top 20 in terms of abundance).

Table 3 Correspondence table between the classification of genus-level microorganisms (top 20 in terms of abundance) and the initial parameters of microorganisms in MSIM.

Table 4 Model state parameters of the multiple linear regression model for quinone profile -microbial populations.

838 **Table 1**

Experimental Group	Day 0	Day 180	Day 360
PCE + Bioaugmentation (BA)	A1	B1	C1
PCE + Natural Attenuation (NA)	A2	B2	C2
PCE + Electron Donors (BS)	A3	B3	C3
PCE + Low concentration Benzene co-contamination (PCE+BZ_L)	A4	B4	C4
PCE + High concentration Benzene co-contamination (PCE+BZ_H)	A5	B5	C5

839

Table 2

No.	Genus-Level Microorganism	BTEX Degradation Ability	CEs Degradation Ability	Oxygen Relationship	References
1	*Pseudomonas*	Yes	Yes	Aerobic	[42,43]
2	*Ralstonia*	Yes	Co-metabolism Related	Anaerobic	[44,45]
3	*Pseudoxanthomonas*	Yes	Unknown	Aerobic	[46]
4	*Arthrobacter*	Yes	Co-metabolism Related	Aerobic	[47,48]
5	*norank_f_Symbiobacteraceae*	Unknown	Unknown	Anaerobic	/
6	*Bradyrhizobium*	Unknown	Unknown	Anaerobic	/
7	*Sediminibacterium*	Unknown	Unknown	Aerobic	/
8	*unclassified_f__Enterobacteriaceae*	Unknown	Unknown	Anaerobic	/
9	*Rhodococcus*	Yes	Co-metabolism Related	Aerobic	[49,50]
10	*Bacillus*	Yes	Co-metabolism Related	Aerobic	[51,52]
11	*Qipengyuania*	Unknown	Unknown	Anaerobic	/
12	*Methylobacterium-Methylorubrum*	Unknown	Unknown	Aerobic	/
13	*Nocardioides*	Yes	Co-metabolism Related	Anaerobic	[53,54]

14	*Desulfurispora*	Unknown	Unknown	Anaerobic	/
15	*Massilia*	Yes	Unknown	Aerobic	[55]
16	*unclassified_f__Oxalobacteraceae*	Unknown	Unknown	Unknown	/
17	*norank_f__TRA3-20*	Unknown	Unknown	Unknown	/
18	*Blastococcus*	Unknown	Unknown	Aerobic	/
19	*Paenibacillus*	Yes	Yes	Aerobic	[56]
20	*Rhodoferax*	Yes	Yes	Anaerobic	[57,58]
21	*others*	/	/	/	/

841

842 **Table 3**

No.	Microbial Community	Genus-Level Microorganism
1	BTEX Degraders, $X_{B, Aer}$	*Pseudomonas*、*Pseudoxanthomonas*、*Arthrobacter*、*Bacillus*、*Massilia*、*Paenibacillus*
2	Aerobic CEs & BTEX Degraders, $X_{B\&C, Aer}$	*Arthrobacter*、*Rhodococcus*、*Bacillus*
3	CEs Degraders, $X_{C, An}$	*Pseudomonas*、*Rhodoferax*
4	Anaerobic CEs & BTEX Degraders, $X_{B\&C, An}$	*Ralstonia*、*Nocardioides*

843

844 **Table 4**

No.	Dependent Variable	Independent Variables	Coefficient of Determination (R^2)	F-Value	p-Value	Durbin-Watson (D-W) Value
1	$X_{B, Aer}$	MK-9, MK-8(H_2), MK-7, MK-7(H_2), MK-6	0.711	1.844	0.020	2.437
2	$X_{B\&C, Aer}$	MK-9, MK-8, MK-8(H_2), MK-7(H_2)	0.646	1.615	0.025	1.774
3	$X_{C, An}$	MK-11, MK-7(H_2), MK-7, MK-9	0.763	3.493	0.004	1.312
4	$X_{B\&C, An}$	UQ-8, MK-8, MK-6, UQ-6	0.709	2.524	0.011	3.128

845

Figure Captions

Fig. 1 Comparison of microbial community composition at the phylum (a) and genus (b) levels across experimental groups.

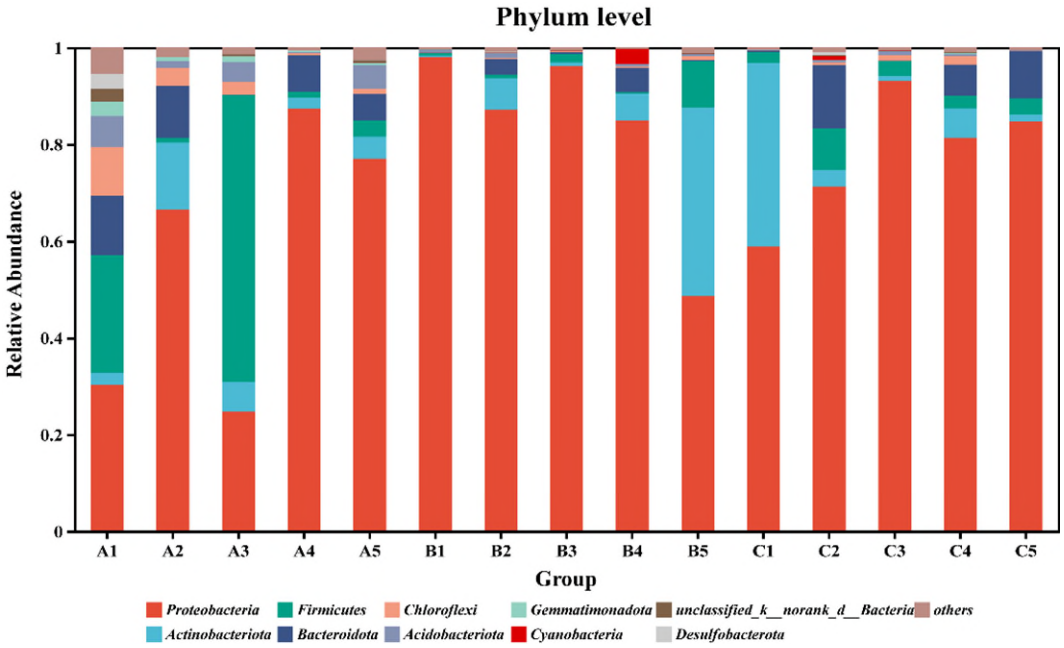
Fig. 2 Distribution of dominant species composition at the phylum (a) and genus (b) levels across different contamination scenario samples.

Fig. 3 Linear regression between total quinone content (TQ) and microbial biomass carbon (MTOC).

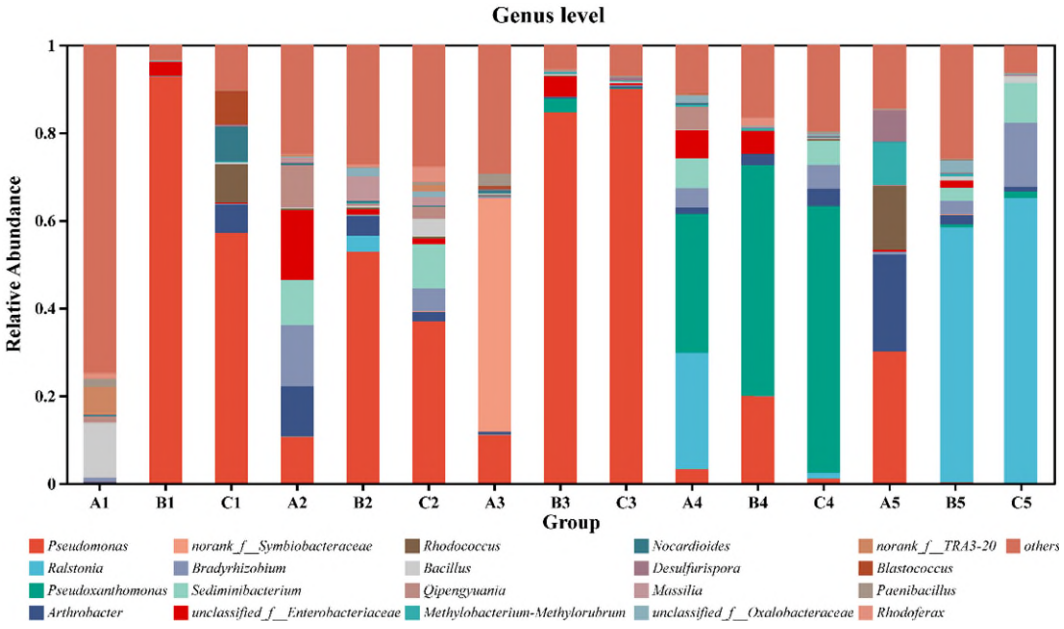
Fig. 4 Correlation analysis between quinone composition and microbial community structure at the phylum level (a) and genus level (b) in microcosm systems.

Fig. 5 Correlation analysis between quinone profiles and microbial populations by degradation function.

Figure 1

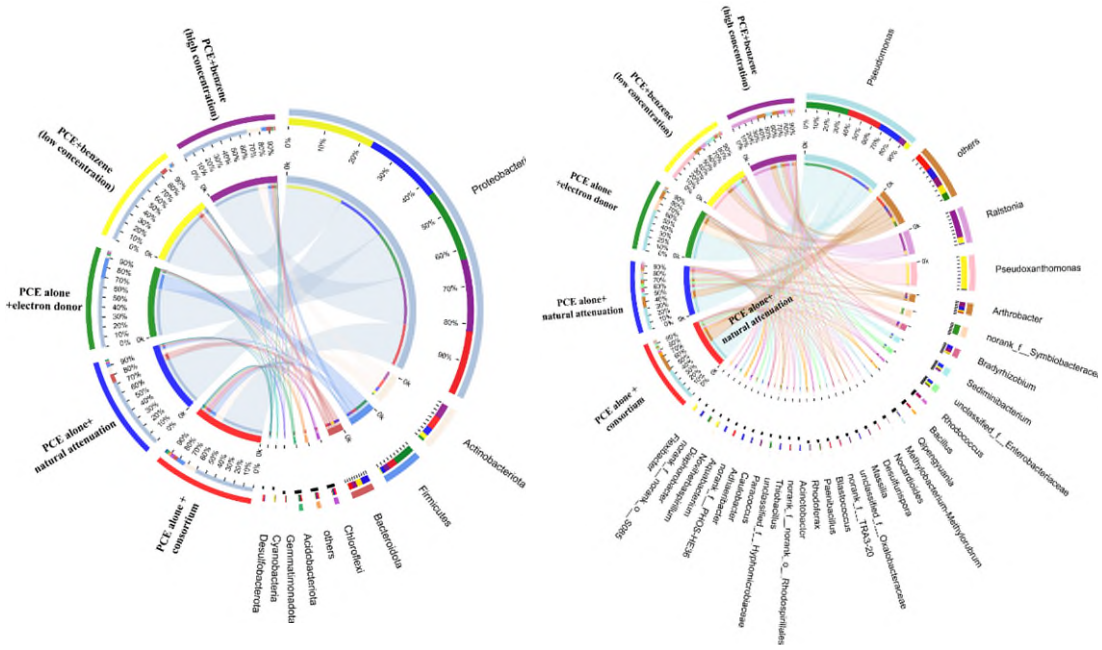

Phylum level
Relative Abundance
1
0.8
0.6
0.4
0.2
0
A1 A2 A3 A4 A5 B1 B2 B3 B4 B5 C1 C2 C3 C4 C5
Group
Proteobacteria
Firmicutes
Chloroflexi
Gemmatimonadota
unclassified_k__norank_d__Bacteria
others
Actinobacteriota
Bacteroidota
Acidobacteriota
Cyanobacteria
Desulfobacterota

(a)


Genus level
Relative Abundance
1
0.8
0.6
0.4
0.2
0
A1 B1 C1 A2 B2 C2 A3 B3 C3 A4 B4 C4 A5 B5 C5
Group
Pseudomonas
norank_f__Symbiobacteraceae
Rhodococcus
Nocardioides
norank_f__TRA3-20
others
Ralstonia
Bradyrhizobium
Bacillus
Desulfurispora
Blastococcus
Pseudoxanthomonas
Sediminibacterium
Qipengyuania
Massilia
Paenibacillus
Arthrobacter
unclassified_f__Enterobacteriaceae
Methylobacterium-Methylorubrum
unclassified_f__Oxalobacteraceae
Rhodoferax

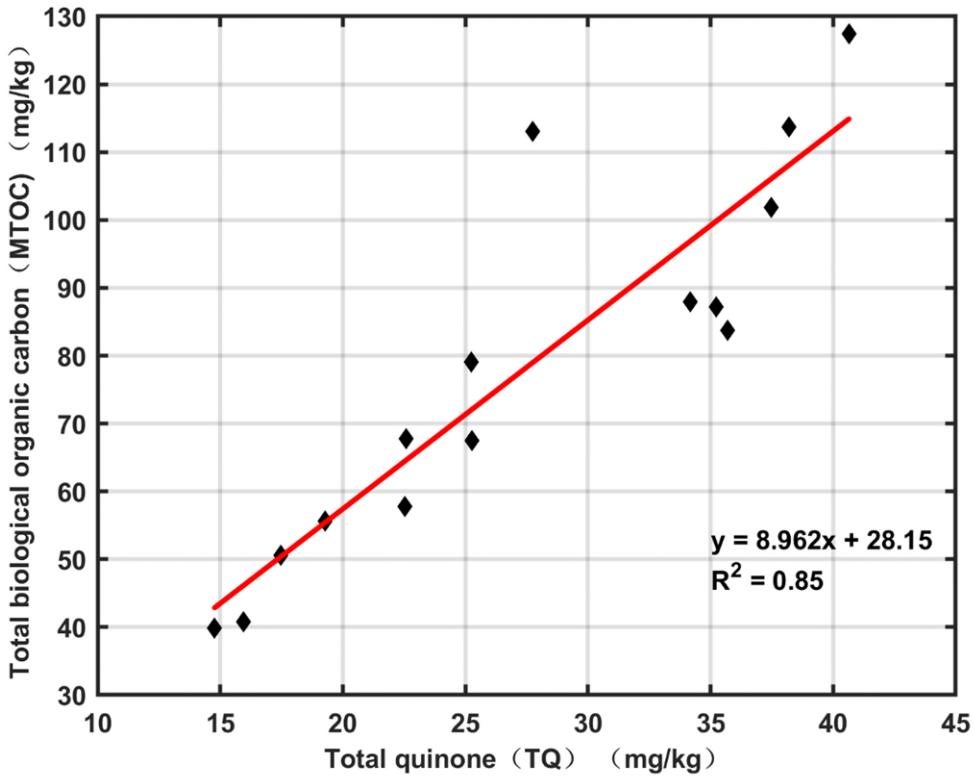
(b)

Figure 2

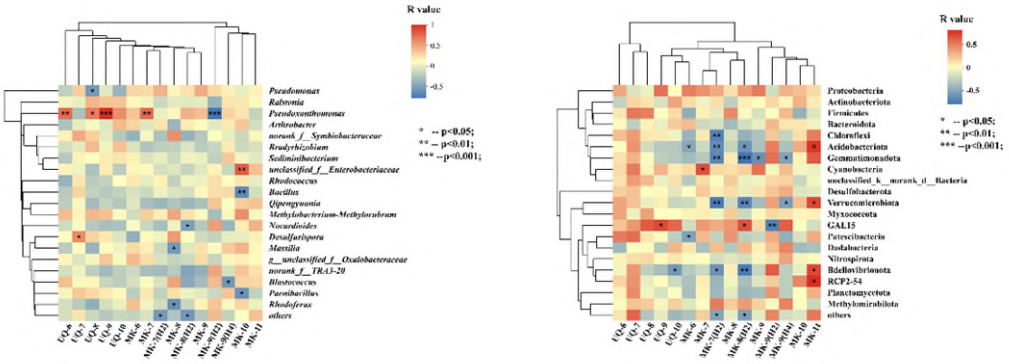

PCE+benzene (high concentration)
PCE+benzene (low concentration)
PCE alone +electron donor
PCE alone+ natural attenuation
PCE alone + consortium
Proteobacteria
Actinobacteriota
Firmicutes
Bacteroidota
Chloroflexi
others
Acidobacteriota
Gemmatimonadota
Cyanobacteria
Desulfobacterota
Pseudomonas
others
Ralstonia
Pseudoxanthomonas
Arthrobacter
norank_f__Symbiobacteraceae
Bradyrhizobium
Sediminibacterium
unclassified_f__Enterobacteriaceae
Rhodococcus
Bacillus
Oxynitrigenia
Methylobacterium-Methylorubrum
Nocardioides
Massilia
Desulfuromonas
unclassified_f__Oxalobacteraceae
norank_f__TRA3-20
Blastococcus
Paenibacillus
Rhodoferax
Acinetobacter
norank_f__norank_o__Rhodospirillales
Thiobacillus
unclassified_f__Hyphomicrobiaceae
Pseudococcus
Gaiellaceae
Aquisediminimonas
norank_f__norank_o__SG8-4
Dechloromonas
Flavobacterium
Pseudarthrobacter

(a) **(b)**

Figure 3


Total biological organic carbon（MTOC)（mg/kg）
Total quinone（TQ） （mg/kg）
y = 8.962x + 28.15
R2 = 0.85
130
120
110
100
90
80
70
60
50
40
30
10
15
20
25
30
35
40
45

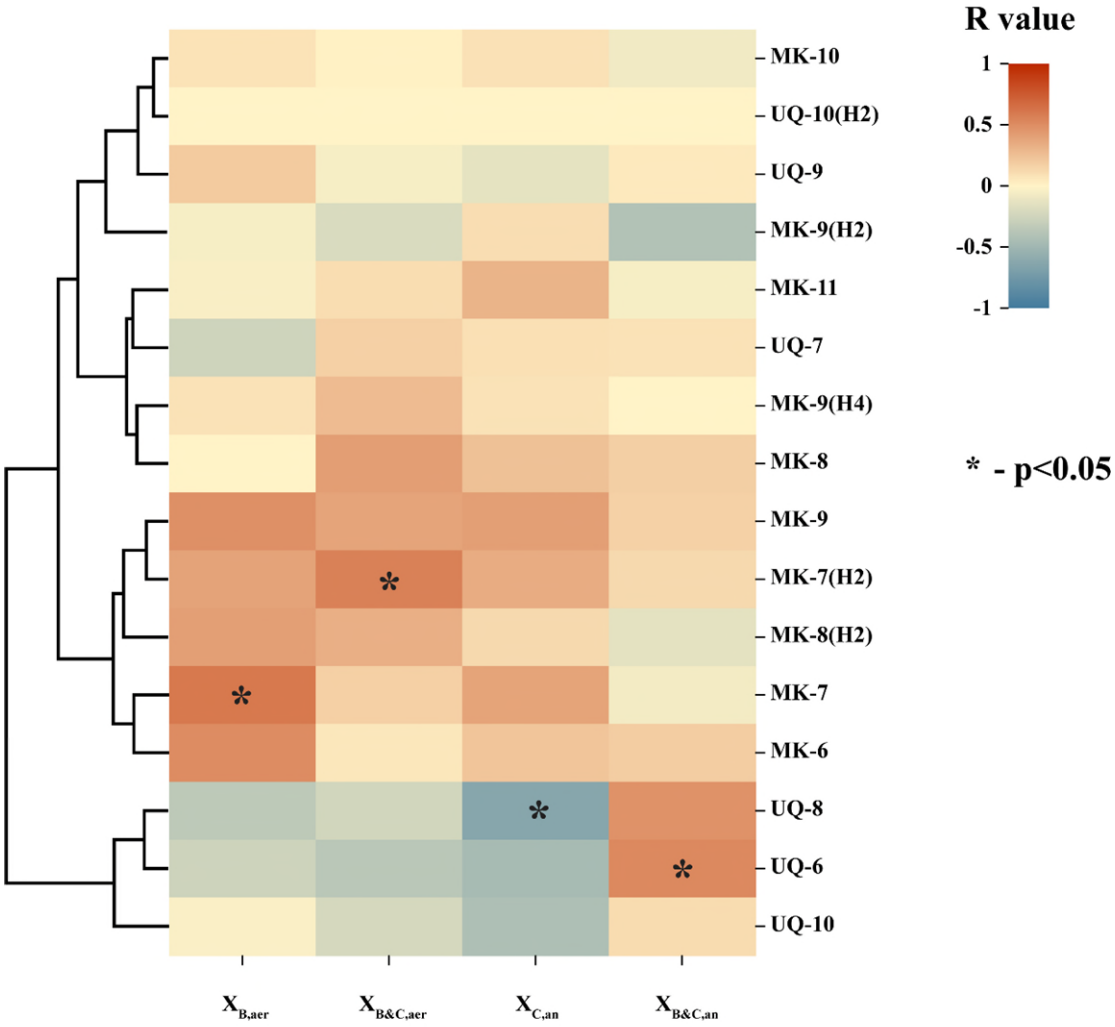
866 **Figure 4**



(a) **(b)**

867

868 **Figure 5**



$X_{B, Aer}$ - Aerobic BTEX degraders;
$X_{B\&C, Aer}$ - Aerobic CEs & BTEX co-degraders;
$X_{C, An}$ - Anaerobic CEs degraders;
$X_{B\&C, An}$ - Anaerobic CEs & BTEX co-degraders.

869

Supplementary Files

This is a list of supplementary files associated with this preprint. Click to download.

- SupportingInformationSIrevision.docx